MiR-1301-3p Inhibits Epithelial-mesenchymal Transition via Targeting RhoA in Pancreatic Cancer

Xinxue Zhang
Zhangyong Ren
Junming Xu
Qing Chen
Jun Ma
Zhe Liu
Jiantao Kou
Xin Zhao
Ren Lang
Qiang He (heqiang@bjcyh.com)

Research Article

Keywords: miR-1301-3p, RhoA, EMT, pancreatic cancer

Posted Date: December 21st, 2021

DOI: https://doi.org/10.21203/rs.3.rs-1147164/v1

Version of Record: A version of this preprint was published at Journal of Oncology on February 26th, 2022. See the published version at https://doi.org/10.1155/2022/5514715.

Abstract

Micro(mi)RNAs play an essential role in the epithelial-mesenchymal transition (EMT) process in human cancers. This study aimed to uncover the regulatory mechanism of miR-1301-3p on EMT in pancreatic cancer (PC). The miRNA profilings from Gene Expression Omnibus datasets (GSE31568, GSE41372, and GSE32688) demonstrated the downregulation of miR-1301-3p in PC tissues, which was validated with 72 paired PC tissue samples through qRT-PCR detection. The low level of miR-1301-3p was associated with a poor prognosis for PC patients from the PC cohort of The Cancer Genome Atlas and the validation cohort. Gene Ontology analyses indicated that the target genes of miR-1301-3p were involved in cell cycle and adherent junction regulation. *In vitro* assays revealed that miR-1301-3p suppressed the proliferation and migration abilities of PC cells. Western blotting and luciferase reporter assays suggested that miR-1301-3p inhibited RhoA expression by targeting its 3'-untranslated region; RhoA upregulated N-cadherin and vimentin level, however, downregulated E-cadherin level. In conclusion, our study showed that miR-1301-3p could serve as a prognostic biomarker for PC and suppress PC cell malignancy by targeting RhoA induced EMT process.

Introduction

Pancreatic cancer (PC) is the fourth leading cause of cancer-related deaths worldwide with a 5-year overall survival (OS) of 5% [1]. Due to the lack of specific symptoms and biomarkers, 50% of patients were diagnosed with PC in the advanced stage and lost the opportunity for radical surgery [2]. Therefore it is crucial to elucidate the signature driver molecules in PC tumorigenesis and progression. Micro(mi)RNA, a small non-coding RNA can degrade the mRNA by binding to the 3'-untranslated region (3'UTR) of the target gene. Accumulating studies have revealed that miRNAs may regulate cancer-associated biological processes such as cell proliferation [3], differentiation [4], apoptosis [5], and epithelial-mesenchymal transition (EMT) [6].

We previously identified the clinically relevant miRNAs through conjoint analyses with multiple miRNA expression profiling data and found that miR-1301-3p were downregulated in PC tissues and the low level of miR-1301-3p was associated with poor OS for PC patients [7]. Recent studies suggest that miR-1301-3p exhibits tumor-suppressive activity in esophageal squamous cell carcinoma [8], papillary thyroid carcinoma [9], and osteosarcoma [10] by interacting with noncoding RNAs. On the contrary, miR-1301-3p is upregulated in gastric cancer tissues and promotes cancer cell proliferation via targeting SIRT1 [11]. These results indicated possible dual regulatory roles of miR-1301-3p in various cancers, however, the effect of miR-1301-3p on PC is unclear and imperative to be discovered.

The purpose of this study was to validate the clinical significance of miR-1301-3p in PC and illustrate its function and potential signal pathway in PC cells.

Materials And Methods

The Differential and Survival Analyses for miR-1301-3p. Firstly, we extracted miR-1301-3p expression data from three PC-miRNA expression profilings (GSE31568, GSE41372, and GSE32688) of the Gene Expression Omnibus (GEO) database. Next, we compared the miR-1301-3p level between PC tissues and normal tissues within the three datasets. To verify the prognostic importance, the clinical data and miR-1301-3p expression value were also obtained through the PC cohort of The Cancer Genome Atlas (TCGA) database. According to the miR-1301-3p median value, we divided PC patients into high- and low-level groups and performed Kaplan-Meier survival analyses. A *P*-value was calculated by the log-rank test.

Patients and Samples in Validation Cohort. Between February 2018 and August 2020, 72 PC patients were enrolled in a validation cohort. These patients had not accepted radiotherapy or chemotherapy preoperatively, and the final diagnosis of PC was determined by pathological results. Surgically resected PC tissues and adjacent normal tissues were immediately stored in liquid nitrogen for two hours and then transferred into a -80 °C refrigerator for storage. Postoperatively, these patients have followed an average of 12 months, ranging from two to 29 months. The ethics committee of Beijing Chao-Yang Hospital approved this study, and all patients signed the informed consent form.

Functional Annotation and Signaling Pathway Enrichment for miR-1301-3p. We first applied the miRWalk2.0 database to predict the binding genes of miR-1301-3p and then performed correlation analyses between mRNA expression of these genes and miR-1301-3p values based on the PC cohort of TCGA. Finally, the genes negatively correlated with miR-1301-3p were regarded as the target genes of miR-1301-3p.

To understand the functions of these target genes, we performed Gene Ontology (GO) and Kyoto Encyclopedia of Genes and Genomes (KEGG) pathway enrichment analyses using the clusterProfiler R package [12]. A protein-protein interaction (PPI) network was constructed using the Search Tool for the Retrieval of Interacting Genes database and visualized with Cytoscape software. The correlation of each PPI relationship pair was represented by a combined score ranging from 0 (low) to 1 (high). In our study, an interaction > 0.4 (moderate) was applied as the cut-off value. The Molecular Complex Detection plug-in in Cytoscape software was used to identify the hub genes among the PPI network. The screening conditions were set as degree cut-off = 2, K-Core = 2, and Node Score Cutoff = 0.2. Besides, we verified the hub gene expression using the PC-mRNA data of GSE16515.

Quantitative Real-Time Polymerase Chain Reaction (qRT-PCR). TRIzol (Invitrogen, USA) was used for total RNA extraction and qualified using the NanoDrop ND-1000 (Thermo Fisher, USA). Total RNA was converted to the first-strand cDNA according to the manufacturer's protocol (rtStarTM First Strand cDNA Synthesis Kit, Arraystar Inc.). Specific primers for miR-1301-3p were designed by RiboBio (Guangzhou, China).The sequence of forward and reverse primers for miR-1301-3p was 5'- ACACTCCAGCTGGGTTGCAGCTGCCTGGGAGT-3' and 5'-CTCAACTGGTGTCGTGGAGTCGGCAATTCAGTTGAGGAAGTCAC-3'. qRT-PCR was performed using Arraystar SYBR® Green Real-time qPCR Master Mix (Arraystar Inc.) according to the manufacturer's

instructions. The relative expression of miR-1301-3p was calculated using the $2^{-\Delta\Delta Ct}$ method and normalized to β-actin expression levels.

Cell Culture and Transfection. Five PC cell lines and one pancreatic cell line were selected to test the expression of miR-1301-3p, including SW1990, AsPC-1, CFPAC-1, PANC-1, Patu-8988, and HPDE6-C7. These cells were purchased from the American Type Culture Collection (Manassas, VA, USA). We cultured these cells with DMEM medium (Biological Industries) containing penicillin/streptomycin and 10% fetal bovine serum (FBS) at 37 °C with 5% CO^2. Since miR-1301-3p was relatively highly expressed in SW1990 and PANC-1 cells (Figure 1e), we selected these two cell lines to conduct further experiments.

MiR-1301-3p mimics, inhibitor, and negative control (NC) were designed and synthesized by RiboBio (Guangzhou, China). Small interference RNA against RhoA (knockdown group, KD) was designed and synthesized by GenePharma (Shanghai, China). The lentiviral vectors encoding RhoA (overexpression group, OE) were constructed by Gene-Chem (Shanghai, China). In brief, miR-1301-3p mimics and inhibitor (100nM) were transfected into PANC-1 and SW1990 cells using Lipofectamine 3000 reagent (Invitrogen, USA), following the manufacturer's instruction.

Cell Counting Kit-8 (CCK-8) assays. According to the manufacturer's instructions, we performed CCK-8 assays (Sigma Aldrich) to examine the proliferation ability of PC cells. Approximately 2×10^3 cells were added to each well of the 96-well plate, and then the plate was cultured for 24h at 37 °C. Next, we added 50μl of the miR-1301-3p mimics, inhibitor, and NC to the wells of the 96-well plate. Then the plate was placed in a 37 °C incubator again for 24h. At 0, 24, 48, 72, and 96h, 10 μl CCK-8 solution was added to each well. After 2h optical density (OD), 450nm values were measured using the enzyme-labeled instrument (Bio-Rad, United States). Cells were tested three times for each group.

Transwell Migration Assays. We conducted transwell migration assays with a chamber with 8 μm pores (Corning, NY, USA). A suspension containing 1×10^4 PANC-1 and SW1990 cells was prepared and suspended separately in serum-free DMEM with mitomycin-C (1 μg/mL) and added into the upper chamber. After that, 500ul of 10% serum-containing DMEM was added into the lower chamber of the well and incubated 24h at 37 °C. After 24h, PC, cells in the upper chamber were removed. Four random fields were selected at 4× magnification for counting cell numbers. Each experiment was performed three times.

Wound Healing Assay. SW1990 and PANC-1 cells (1×10^5) were incubated in six-well culture plates for 48h until the cells were 80-90% confluent. Cells were maintained in 10% FBS containing DMEM media for 24 hours. PBS was used to wash away the non-adherent cells. A sterile 200-μl pipet was used to make a scratch in the center of the cell monolayer. The monolayer was washed three times with PBS, and fresh media was added. After 0h, 24h, and 48h, the wound width was measured at 2.5× magnification. Each assay was performed three times.

Protein extraction and Western Blotting Assays. Total protein was extracted from PC cells after 72h transfection, and the BCA protein assay kit (Beyotime, China) was used to measure protein concentration,

followed by the manufacturer's instructions. Briefly, 12% SDS-PAGE was used for electrophoresis, and then the proteins were transferred to PVDF membranes. GAPDH, RhoA, E-cadherin, N-cadherin, and vimentin antibodies were used to analyze total protein. Specific primary rabbit anti-human antibodies (CST, 1:1000) were used to incubate the membranes at 4°C overnight. On the second day, the membranes were incubated with HRP-conjugated anti-rabbit IgG antibodies (1:2000) at room temperature for 1h. An enhanced chemiluminescence detection system was used to visualize the bands. GAPDH was used as an internal control. Rabbit anti-GAPDH, RHOA, N-cadherin, E-cadherin, and vimentin antibodies (Cell Signaling Technology, Danvers, MA, USA) were used to analyze cell lysates.

Luciferase Reporter Assays. According to the starBase network tool, RhoA is a predicted target for miR-1301-3p. The binding site between miR-1301-3p and 3'UTR of RhoA was evaluated by using the pmirGLO dual-luciferase miRNA expression vector containing wild type (WT) or mutant (MUT) 3'UTR of RhoA. The WT or MUT 3'UTR of RhoA and miR-1301-3p mimics were co-transfected into PANC-1 cells. After 48h, the luciferase reporter assay system was used to examine the luciferase activity. Each experiment was performed in triplicate.

Immunohistochemistry Analyses. We applied immunohistochemistry assays to validate RhoA expression level in PC tissues. In brief, we sectioned the paraffin-embedded tissue specimens and incubated them with anti-RhoA primary antibody (1:200; ZSGB-BIO, Beijing, China) overnight at 4 °C. The slides were incubated with HRP-conjugated secondary antibody (goat anti-rabbit IgG; BOSTER, Hangzhou, China) for 1h. To visualize the RhoA, 3,3'Diaminobenzidine substrate solution was used as the chromogen.

Statistical Analysis. R software version 3.6.0 was used to perform statistical analyses. Continuous variables between the two groups were compared by a paired sample *t*-test. The data were presented as the mean ± standard deviation. Qualitative data were analyzed by the chi-square test. Fisher's exact test was employed to compare the categorical variables among groups. GraphPad Prism 8.0 (GraphPad Software, inc. La Jolla, CA, USA) was applied to produce figures. *P*-value < 0.05 was considered statistically significant.

Results

MiR-1301-3p Is Downregulated in PC Tissues and Its Low Level Is Correlated with A Poor Prognosis for PC Patients. Based on miRNA microarray data (GSE31568, GSE 41372, GSE32688), the miR-1301-3p was significantly downregulated in PC tissues, compared with normal tissues (Figure 1a-c). In the validation cohort, miR-1301-3p level was lower in PC tissues than in healthy tissues through qRT-PCR detection (Figure 1d). As shown in Figure 1e, the miR-1301-3p level was relatively higher in the pancreatic cell than in PC cells. Furthermore, the miR-1301-3p low level was associated with poor OS in the PC cohort of TCGA and the validation cohort (Figure 1f and g). The univariate analyses showed that miR-1301-3p low level was related to malignant pathological differentiation, tumor residual, and lymphatic metastasis in PC patients (Table 1).

MiR-1301-3p Inhibits the Proliferation and Migration Abilities of Pancreatic Cancer Cells. CCK-8 assays showed that PC cell proliferation was suppressed after miR-1301-3p mimics transfection (Figure 2a). Wound healing assays demonstrated that the migration ability of PC cells was lower in the miR-1301-3p mimics group than that in the NC group (Figure 2b). Similarly, transwell assays supported that miR-1301-3p mimics downregulated PC cell migration ability (Figure 2c). In addition, rescue experiments revealed that inhibiting effect of miR-1301-3p on cell migration was reserved by RhoA overexpression (Figure 2d).

GO Annotation and KEGG Pathway Enrichment for MiR-1301-3p. To uncover the potential functions of miR-1301-3p, we screened out 35 target genes of miR-1301-3p and performed bioinformatics analyses. The GO analyses showed that the target genes of miR-1301-3p were enriched in positive regulation of cell cycle, TGF-β receptor signaling pathway, and cellular response to TGF-β stimulus in the biological process (Figure 3a). In terms of cellular components, the target genes were associated with adherens junction, focal adhesion, and cell-substrate junctions (Figure 3b). In terms of molecular functions, the target genes were mostly enriched in anion transmembrane transporter activity and guanyl nucleotide binding (Figure 3c). The KEGG pathway analyses displayed that the target genes of miR-1301-3p were mainly enriched in the phospholipase D signaling pathway and Ras signaling pathway (Figure 3d). These results suggested that miR-1301-3p was probably associated with the regulation of cell migration and proliferation.

MiR-1301-3p Inhibits RhoA Induced Epithelial-Mesenchymal Transition. We performed PPI analyses to screen out the pivotal gene in the 35 target genes of miR-1301-3p. After that, RhoA was identified as a hub gene in the PPI network (Figure 4a). Specially, RhoA is involved in cellular junction and TGF-β receptor signaling pathway according to the GO and KEGG analyses, which were driving factors in tumor progression. Therefore, we selected RhoA to conduct the following validation experiments. As shown in Figure 4b, miR-1301-3p negatively correlated with RhoA expression in the PC cohort of TCGA. Through the starBase network tool, the binding site was identified between miR-1301-3p and RhoA 3'UTR (Figure 4c). Moreover, luciferase reporter assays showed that miR-1301-3p mimics significantly downregulated the relative luciferase activity of RhoA-WT in PANC-1 cells (Figure 4c). Besides, WB assays showed that miR-1301-3p mimics decreased RhoA protein expression, while miR-1301-3p inhibitor increased RhoA level in PANC-1 and SW1990 cells (Figure 4d). Immunohistochemical examination indicated that RhoA staining was heavier in miR-1301-3p low-level PC tissue than in high-level PC tissue (Figure 4e).

Subsequently, we revealed that N-cadherin and vimentin expression levels were downregulated in the RhoA knockdown group than those in the NC group; in contrast, E-cadherin level was upregulated in the RhoA knockdown group (Figure 5a). On the contrary, overexpression of RhoA increased N-cadherin and vimentin levels, however, decreased E-cadherin level in PANC-1 and SW1990 cells (Figure 5a). Further rescue experiments showed that RhoA overexpression could abolish the suppression of EMT process due to miR-1301-3p mimics (Figure 5b). Taken together, these results suggested that miR-1301-3p could inhibit RhoA-induced EMT in PC cells.

Discussion

Accumulated evidence has pointed out that miRNAs can contribute a crucial regulatory role in PC tumorigenesis and progression. Here, we revealed that miR-1301-3p was downregulated in PC tissues and its low level was related to the poor overall survival of PC patients. We also found that miR-1301-3p inhibited PC cell proliferation and migration abilities; mechanically, miR-1301-3p could suppress RhoA mediated EMT process in PC cells. Thus, our study provided a new molecular biomarker and a therapeutic target for PC treatment.

We reveal that the high level of miR-1301-3p is associated with good pathological differentiation, fewer infiltrating lymph nodes, and R0 resection in the current study. To our knowledge, we first discovered that miR-1301-3p may serve as a tumor suppressor in PC, combined with the results of *in vitro* assays. Generally, the growth of solid tumor relays on the tumor microenvironment which contains the complicated interactions between multiple stromal cells and the extracellular matrix. Thus, we failed to reveal that the overexpression of miR-1301-3p was related to smaller PC tumor, although *in vitro* assays suggested that miR-1301-3p suppressed PC cells proliferation.

GO analyses indicated that RhoA, a predicted target gene of miR-1301-3p, was involved in the terms of “TGF-β receptor signaling pathway,” “positive regulation of cell cycle,” “cellular response to TGF-β stimulus,” “focal adhesion,” and “myosin binding”. These GO terms suggested that miR-1301-3p possibly regulated cell proliferation and migration process via RhoA. Furthermore, RhoA was involved in “Ras signaling pathway” and “regulation of actin cytoskeleton” in KEGG enrichment analyses, which suggested that RhoA was linked to cell invasion ability. Therefore, we selected RhoA as a functional target gene of miR-1301-3p and conducted subsequent assays.

RhoA is a member of the Rho GTPase family, containing a GTP-bound active form and a GDP inactive part, which can promote actin cytoskeleton reorganization and regulate cell shape, attachment, and motility [13, 14]. The RhoA overexpression is associated with PC cell growth and metastasis. For example, KRas activation upregulated eIF5A level, which promoted PC cells motility and metastasis via Rho/ROCK [15]; cyclic AMP could decrease RhoA level and inhibited PC cell migration and invasion [16]; crizotinib, a MET antibody could downregulate RhoA level and suppress PC cell invasiveness [17].

A critical step of tumor metastasis is known as the EMT process, in which cancer cells lose their polarities and cellular connections, and acquire migration ability [18, 19]. This process is characterized by loss of the cell adhesion protein, E-cadherin, and upregulation of N-cadherin and vimentin, representing mesenchymal phenotypes. It has been proven that EMT-activators promote tumor development in multiple human cancers [20-23]. Activation of the RhoA/ROCK signaling pathway may upregulate the EMT process. Notably, RhoA was reported to facilitate the EMT process in gastric cancer and esophagus cancer [24, 25]; however, the association between EMT and RhoA is unclear in PC. In this study, we provided evidence that RhoA activation promoted the EMT process in PC cells. Interestingly, several miRNAs could also downregulate RhoA, for example: miR-154-3p and miR-487-3p specifically repressed RhoA expression and blocked thyroid cancer cell growth [26]; miR-101 downregulated EMT process and breast cancer cell migration by reducing RhoA level [27].

In summary, we revealed that miR-1301-3p could serve as a prognostic biomarker for PC. Overexpression of miR-1301-3p inhibits PC cell proliferation, and migration. Mechanistically, miR-1301-3p suppresses RhoA induced EMT process, and thus, miR-1301-3p/RhoA could be a novel target for PC treatment.

Declarations

ACKNOWLEDGMENTS

We thank Drs. Hua Fan, Xianliang Li, Yu Liu, and Lixin Li for general support and for providing samples.

AUTHOR CONTRIBUTIONS

The conception and design of the study, as well as manuscript writing, were performed by Xinxue Zhang and Xin Zhao; administrative support was provided by Qiang He; the provision of study materials was by Ren Lang; the collection and assembly of data were by Jun Ma and Jiantao Kou; the experiments were performed by Zhe Liu and Junming Xu. All authors read and approved the final manuscript.

ADDITIONAL INFORMATION

Ethics approval and consent to participate The Research Ethics Committee of Beijing Chao-Yang Hospital affiliated to Capital Medical University approved the use of anonymized human pancreatic cancer samples.

Availability of data and materials not applicable.

Competing Interests, The authors disclose no potential conflicts of interest.

References

1. Siegel R, Ma J, Zou Z, Jemal A. Cancer statistics, 2014. CA Cancer J Clin 2014; 64: 9-29.

2. Mizrahi JD, Surana R, Valle JW, Shroff RT. Pancreatic cancer. Lancet 2020; 395: 2008-2020.

3. Zhang J, He J, Zhang L. The down-regulation of microRNA-137 contributes to the up-regulation of retinoblastoma cell proliferation and invasion by regulating COX-2/PGE2 signaling. Biomed Pharmacother 2018; 106: 35-42.

4. Otto T, Candido SV, Pilarz MS et al. Cell cycle-targeting microRNAs promote differentiation by enforcing cell-cycle exit. Proc Natl Acad Sci U S A 2017; 114: 10660-10665.

5. Zhu L, Xue F, Xu X et al. MicroRNA-198 inhibition of HGF/c-MET signaling pathway overcomes resistance to radiotherapy and induces apoptosis in human non-small-cell lung cancer. J Cell Biochem 2018; 119: 7873-7886.

6. Alidadiani N, Ghaderi S, Dilaver N et al. Epithelial mesenchymal transition Transcription Factor (TF): The structure, function and microRNA feedback loop. Gene 2018; 674: 115-120.

7. Zhang Z, Pan B, Lv S et al. Integrating MicroRNA Expression Profiling Studies to Systematically Evaluate the Diagnostic Value of MicroRNAs in Pancreatic Cancer and Validate Their Prognostic Significance with the Cancer Genome Atlas Data. Cell Physiol Biochem 2018; 49: 678-695.

8. Zhang C, Xie L, Fu Y et al. lncRNA MIAT promotes esophageal squamous cell carcinoma progression by regulating miR-1301-3p/INCENP axis and interacting with SOX2. J Cell Physiol 2020; 235: 7933-7944.

9. Wen J, Wang H, Dong T et al. STAT3-induced upregulation of lncRNA ABHD11-AS1 promotes tumour progression in papillary thyroid carcinoma by regulating miR-1301-3p/STAT3 axis and PI3K/AKT signalling pathway. Cell Prolif 2019; 52: e12569.

10. Wang X, Hu K, Chao Y, Wang L. LncRNA SNHG16 promotes proliferation, migration and invasion of osteosarcoma cells by targeting miR-1301/BCL9 axis. Biomed Pharmacother 2019; 114: 108798.

11. Luo D, Fan H, Ma X et al. miR-1301-3p Promotes Cell Proliferation and Facilitates Cell Cycle Progression via Targeting SIRT1 in Gastric Cancer. Front Oncol 2021; 11: 664242.

12. Yu G, Wang LG, Han Y, He QY. clusterProfiler: an R package for comparing biological themes among gene clusters. OMICS 2012; 16: 284-287.

13. Itoh K, Yoshioka K, Akedo H et al. An essential part for Rho-associated kinase in the transcellular invasion of tumor cells. Nat Med 1999; 5: 221-225.

14. Sahai E, Marshall CJ. RHO-GTPases and cancer. Nat Rev Cancer 2002; 2: 133-142.

15. Fujimura K, Choi S, Wyse M et al. Eukaryotic Translation Initiation Factor 5A (EIF5A) Regulates Pancreatic Cancer Metastasis by Modulating RhoA and Rho-associated Kinase (ROCK) Protein Expression Levels. J Biol Chem 2015; 290: 29907-29919.

16. Zimmerman NP, Roy I, Hauser AD et al. Cyclic AMP regulates the migration and invasion potential of human pancreatic cancer cells. Mol Carcinog 2015; 54: 203-215.

17. Takiguchi S, Inoue K, Matsusue K et al. Crizotinib, a MET inhibitor, prevents peritoneal dissemination in pancreatic cancer. Int J Oncol 2017; 51: 184-192.

18. Das V, Bhattacharya S, Chikkaputtaiah C et al. The basics of epithelial-mesenchymal transition (EMT): A study from a structure, dynamics, and functional perspective. J Cell Physiol 2019.

19. Kalluri R, Weinberg RA. The basics of epithelial-mesenchymal transition. J Clin Invest 2009; 119: 1420-1428.

20. Canel M, Serrels A, Frame MC, Brunton VG. E-cadherin-integrin crosstalk in cancer invasion and metastasis. J Cell Sci 2013; 126: 393-401.

21. Labernadie A, Kato T, Brugues A et al. A mechanically active heterotypic E-cadherin/N-cadherin adhesion enables fibroblasts to drive cancer cell invasion. Nat Cell Biol 2017; 19: 224-237.

22. Richardson AM, Havel LS, Koyen AE et al. Vimentin Is Required for Lung Adenocarcinoma Metastasis via Heterotypic Tumor Cell-Cancer-Associated Fibroblast Interactions during Collective Invasion. Clin Cancer Res 2018; 24: 420-432.

23. Padmanaban V, Krol I, Suhail Y et al. E-cadherin is required for metastasis in multiple models of breast cancer. Nature 2019; 573: 439-444.

24. Xu Z, Gu C, Yao X et al. CD73 promotes tumor metastasis by modulating RICS/RhoA signaling and EMT in gastric cancer. Cell Death Dis 2020; 11: 202.

25. Zhu P, Yu H, Zhou K et al. 3,3'-Diindolylmethane modulates aryl hydrocarbon receptor of esophageal squamous cell carcinoma to reverse epithelial-mesenchymal transition through repressing RhoA/ROCK1-mediated COX2/PGE2 pathway. J Exp Clin Cancer Res 2020; 39: 113.

26. Fan XD, Luo Y, Wang J, An N. miR-154-3p and miR-487-3p synergistically modulate RHOA signaling in the carcinogenesis of thyroid cancer. Biosci Rep 2020; 40.

27. Chandra Mangalhara K, Manvati S, Saini SK et al. ERK2-ZEB1-miR-101-1 axis contributes to epithelial-mesenchymal transition and cell migration in cancer. Cancer Lett 2017; 391: 59-73.

Tables

Table 1 not available with this version.

Figures

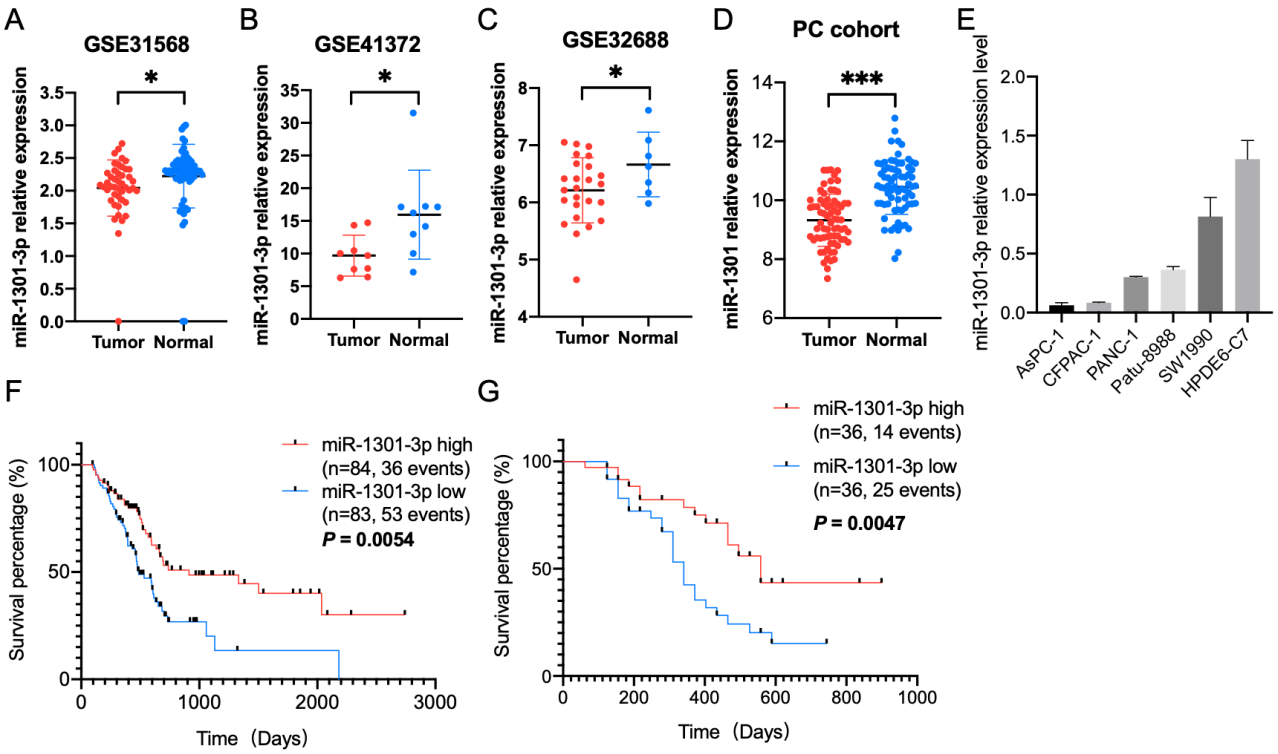

Figure 1

MiR-1301-3p was downregulated in PC tissues and the low level of miR-1301-3p was associated with a poor prognosis for PC patients. (a-c) The miR-1301-3p expression level in PC tissues and the adjacent normal tissues in GSE31568, GSE41372, and GSE32688 datasets. (d) MiR-1301-3p expression level of the validation dataset determined by qRT-PCR. (e) The relative miR-1301-3p expression level of normal pancreatic cell and PC cell lines. (f and g) The correlation between the miR-1301-3p level and the overall survival of PC patients from the PC cohort of TCGA and the validation cohort. *P<0.05, ***P<0.001.

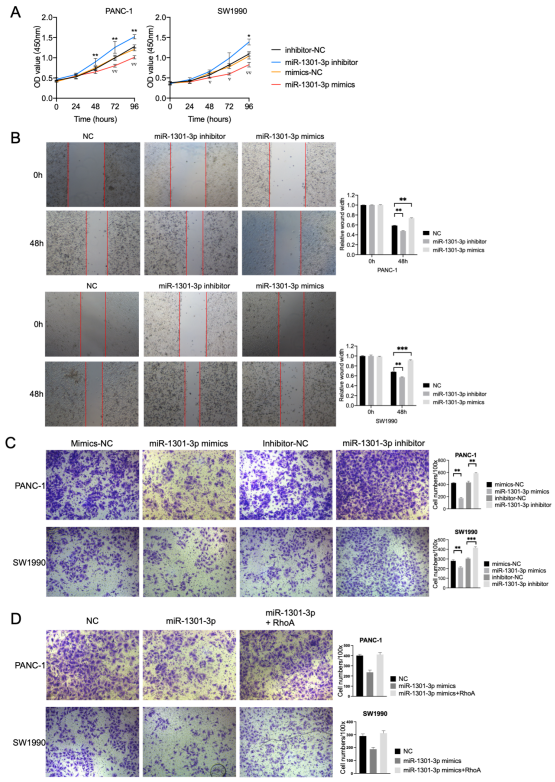

Figure 2

MiR-1301-3p inhibited the proliferation and migration ability of PC cells. (a) CCK-8 assays of PANC-1 and SW1990 cells transfected with miR-1301-3p mimics and inhibitor. (b) Wound healing assays of PANC-1 and SW1990 cells transfected with miR-1301-3p mimics and inhibitor. (c) Transwell migration assays of PANC-1 and SW1990 cells transfected with miR-1301-3p mimics and inhibitor. (d) Transwell migration assays of PANC-1 and SW1990 cells. Data were presented as the mean ± SD of three independent experiments. *P<0.05, **P<0.01, ***P<0.001, ▽P<0.05, ▽▽P<0.01.

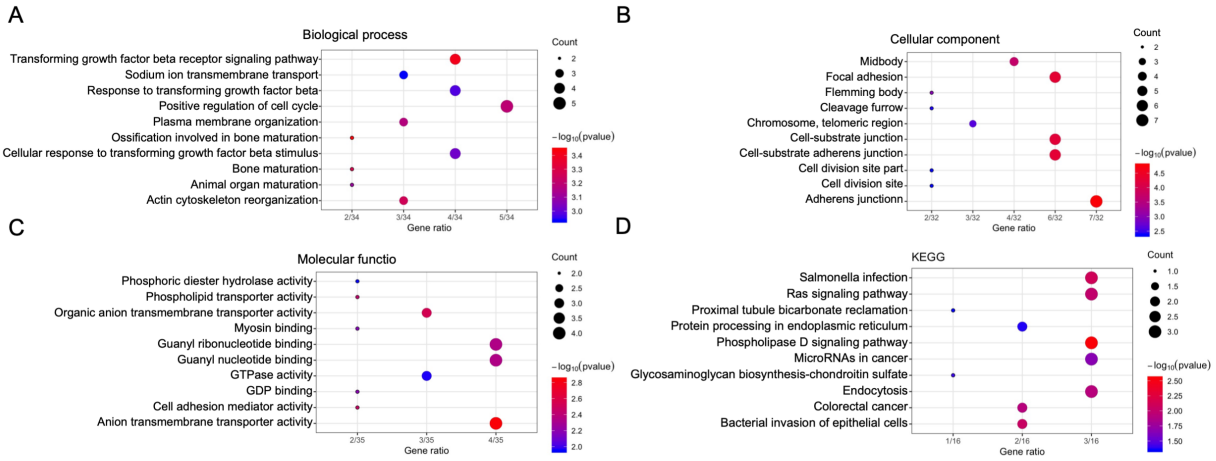

Figure 3

Functional annotation and pathway enrichment analysis of the target genes of miR-1301-3p. (a-c) Gene Ontology terms of biological process, cellular component, and molecular function. (d) Kyoto Encyclopedia of Gene and Genomes pathway enrichment for the miR-1301-3p target genes.

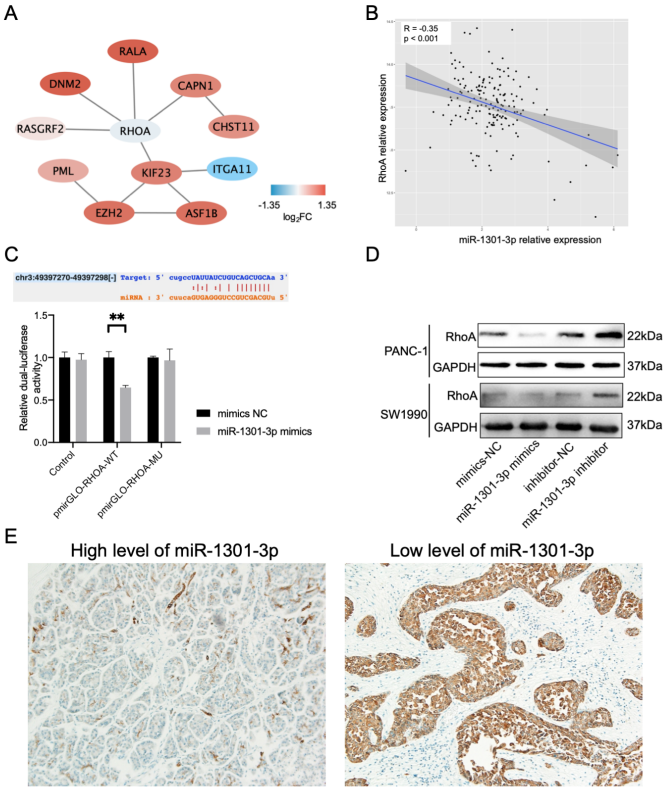

Figure 4

MiR-1301-3p suppressed RhoA expression in PC cells. (a) A protein-protein interaction network showed that RhoA acted as a hub gene among the miR-1301-3p target genes. (b) A negative correlation between miR-1301-3p and RhoA expression level according to the PC cohort of TCGA. (c) Luciferase reporter assays demonstrated that miR-1301-3p was directly bound to the 3'UTR of RhoA in PANC-1 cells. (d) Western blotting assays showed that miR-1301-3p downregulated RhoA expression in PANC-1 and SW1990 cells. (e) The typical immunohistochemical staining of RhoA in miR-1301-3p-upregulated and -downregulated PC tissues.

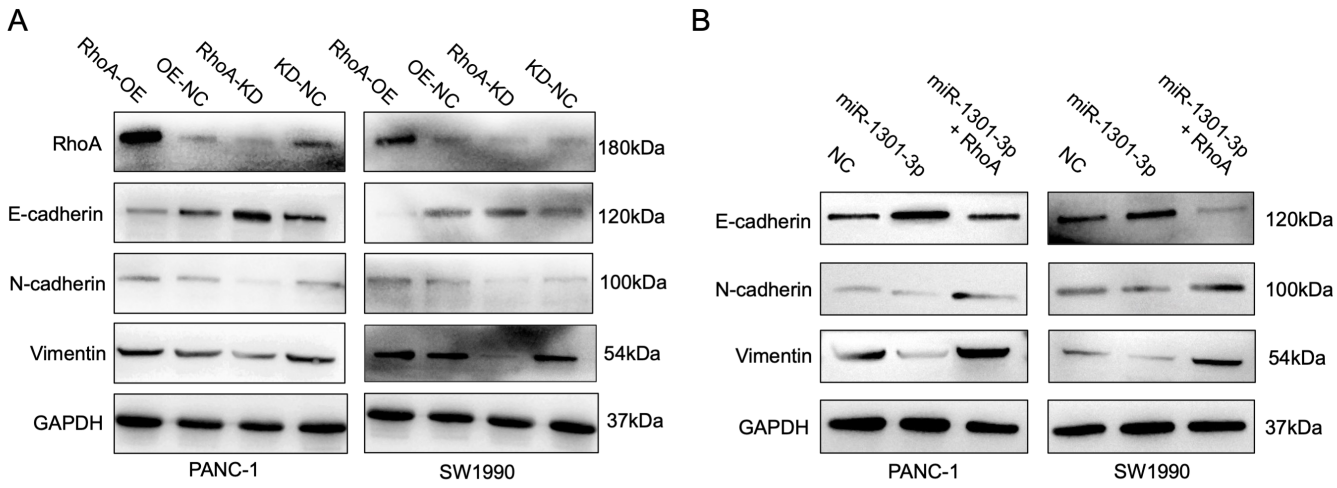

Figure 5

miR-1301-3p inhibited the epithelial-mesenchymal transition process via RhoA in PC cells. (a) The overexpression of RhoA upregulated N-cadherin and vimentin expression level, however, downregulated E-cadherin in PANC-1 and SW1990 cells. In contrast, RhoA knockdown downregulated N-cadherin and vimentin, however, upregulated E-cadherin level. (b) Western blotting assays showing the expression of E-cadherin, N-cadherin, and vimentin in pancreatic cancer cells.